Proton-Λ correlations in central Au+Au collisions at $\sqrt{s_{NN}} = 200$ GeV

J. Adams,[3] M. M. Aggarwal,[29] Z. Ahammed,[44] J. Amonett,[20] B. D. Anderson,[20] D. Arkhipkin,[13] G. S. Averichev,[12] S. K. Badyal,[19] Y. Bai,[27] J. Balewski,[17] O. Barannikova,[32] L. S. Barnby,[3] J. Baudot,[18] S. Bekele,[28] V. V. Belaga,[12] A. Bellingeri-Laurikainen,[39] R. Bellwied,[47] J. Berger,[14] B. I. Bezverkhny,[49] S. Bharadwaj,[34] A. Bhasin,[19] A. K. Bhati,[29] V. S. Bhatia,[29] H. Bichsel,[46] J. Bielcik,[49] J. Bielcikova,[49] A. Billmeier,[47] L. C. Bland,[4] C. O. Blyth,[3] S.-L. Blyth,[21] B. E. Bonner,[35] M. Botje,[27] A. Boucham,[39] J. Bouchet,[39] A. V. Brandin,[25] A. Bravar,[4] M. Bystersky,[11] R. V. Cadman,[1] X. Z. Cai,[38] H. Caines,[49] M. Calderón de la Barca Sánchez,[17] J. Castillo,[21] O. Catu,[49] D. Cebra,[7] Z. Chajecki,[28] P. Chaloupka,[11] S. Chattopadhyay,[44] H. F. Chen,[37] J. H. Chen,[38] Y. Chen,[8] J. Cheng,[42] M. Cherney,[10] A. Chikanian,[49] H. A. Choi,[33] W. Christie,[4] J. P. Coffin,[18] T. M. Cormier,[47] M. R. Cosentino,[36] J. G. Cramer,[46] H. J. Crawford,[6] D. Das,[44] S. Das,[44] M. Daugherity,[41] M. M. de Moura,[36] T. G. Dedovich,[12] M. DePhillips,[4] A. A. Derevschikov,[31] L. Didenko,[4] T. Dietel,[14] S. M. Dogra,[19] W. J. Dong,[8] X. Dong,[37] J. E. Draper,[7] F. Du,[49] A. K. Dubey,[15] V. B. Dunin,[12] J. C. Dunlop,[4] M. R. Dutta Mazumdar,[44] V. Eckardt,[23] W. R. Edwards,[21] L. G. Efimov,[12] V. Emelianov,[25] J. Engelage,[6] G. Eppley,[35] B. Erazmus,[39] M. Estienne,[39] P. Fachini,[4] J. Faivre,[18] R. Fatemi,[22] J. Fedorisin,[12] K. Filimonov,[21] P. Filip,[11] E. Finch,[49] V. Fine,[4] Y. Fisyak,[4] K. S. F. Fornazier,[36] J. Fu,[42] C. A. Gagliardi,[40] L. Gaillard,[3] J. Gans,[49] M. S. Ganti,[44] F. Geurts,[35] V. Ghazikhanian,[8] P. Ghosh,[44] J. E. Gonzalez,[8] H. Gos,[45] O. Grachov,[47] O. Grebenyuk,[27] D. Grosnick,[43] S. M. Guertin,[8] Y. Guo,[47] A. Gupta,[19] N. Gupta,[19] T. D. Gutierrez,[7] T. J. Hallman,[4] A. Hamed,[47] D. Hardtke,[21] J. W. Harris,[49] M. Heinz,[2] T. W. Henry,[40] S. Hepplemann,[30] B. Hippolyte,[18] A. Hirsch,[32] E. Hjort,[21] G. W. Hoffmann,[41] M. J. Horner,[21] H. Z. Huang,[8] S. L. Huang,[37] E. W. Hughes,[5] T. J. Humanic,[28] G. Igo,[8] A. Ishihara,[41] P. Jacobs,[21] W. W. Jacobs,[17] M. Jedynak,[45] H. Jiang,[8] P. G. Jones,[3] E. G. Judd,[6] S. Kabana,[2] K. Kang,[42] M. Kaplan,[9] D. Keane,[20] A. Kechechyan,[12] V. Yu. Khodyrev,[31] B. C. Kim,[33] J. Kiryluk,[22] A. Kisiel,[45] E. M. Kislov,[12] J. Klay,[21] S. R. Klein,[21] D. D. Koetke,[43] T. Kollegger,[14] M. Kopytine,[20] L. Kotchenda,[25] K. L. Kowalik,[21] M. Kramer,[26] P. Kravtsov,[25] V. I. Kravtsov,[31] K. Krueger,[1] C. Kuhn,[18] A. I. Kulikov,[12] A. Kumar,[29] R. Kh. Kutuev,[13] A. A. Kuznetsov,[12] M. A. C. Lamont,[49] J. M. Landgraf,[4] S. Lange,[14] F. Laue,[4] J. Lauret,[4] A. Lebedev,[4] R. Lednicky,[12] C.-H. Lee,[33] S. Lehocka,[12] M. J. LeVine,[4] C. Li,[37] Q. Li,[47] Y. Li,[42] G. Lin,[49] S. J. Lindenbaum,[26] M. A. Lisa,[28] F. Liu,[48] H. Liu,[37] J. Liu,[35] L. Liu,[48] Q. J. Liu,[46] Z. Liu,[48] T. Ljubicic,[4] W. J. Llope,[35] H. Long,[8] R. S. Longacre,[4] M. Lopez-Noriega,[28] W. A. Love,[4] Y. Lu,[48] T. Ludlam,[4] D. Lynn,[4] G. L. Ma,[38] J. G. Ma,[8] Y. G. Ma,[38] D. Magestro,[28] S. Mahajan,[19] D. P. Mahapatra,[15] R. Majka,[49] L. K. Mangotra,[19] R. Manweiler,[43] S. Margetis,[20] C. Markert,[20] L. Martin,[39] J. N. Marx,[21] H. S. Matis,[21] Yu. A. Matulenko,[31] C. J. McClain,[1] T. S. McShane,[10] F. Meissner,[21] Yu. Melnick,[31] A. Meschanin,[31] M. L. Miller,[22] N. G. Minaev,[31] C. Mironov,[20] A. Mischke,[27] D. K. Mishra,[15] J. Mitchell,[35] B. Mohanty,[44] L. Molnar,[32] C. F. Moore,[41] D. A. Morozov,[31] M. G. Munhoz,[36] B. K. Nandi,[44] S. K. Nayak,[19] T. K. Nayak,[44] J. M. Nelson,[3] P. K. Netrakanti,[44] V. A. Nikitin,[13] L. V. Nogach,[31] S. B. Nurushev,[31] G. Odyniec,[21] A. Ogawa,[4] V. Okorokov,[25] M. Oldenburg,[21] D. Olson,[21] S. K. Pal,[44] Y. Panebratsev,[12] S. Y. Panitkin,[4] A. I. Pavlinov,[47] T. Pawlak,[45] T. Peitzmann,[27] V. Perevoztchikov,[4] C. Perkins,[6] W. Peryt,[45] V. A. Petrov,[47] S. C. Phatak,[15] R. Picha,[7] M. Planinic,[50] J. Pluta,[45] N. Porile,[32] J. Porter,[46] A. M. Poskanzer,[21] M. Potekhin,[4] E. Potrebenikova,[12] B. V. K. S. Potukuchi,[19] D. Prindle,[46] C. Pruneau,[47] J. Putschke,[21] G. Rakness,[30] R. Raniwala,[34] S. Raniwala,[34] O. Ravel,[39] R. L. Ray,[41] S. V. Razin,[12] D. Reichhold,[32] J. G. Reid,[46] J. Reinnarth,[39] G. Renault,[39] F. Retiere,[21] A. Ridiger,[25] H. G. Ritter,[21] J. B. Roberts,[35] O. V. Rogachevskiy,[12] J. L. Romero,[7] A. Rose,[21] C. Roy,[39] L. Ruan,[37] M. J. Russcher,[27] R. Sahoo,[15] I. Sakrejda,[21] S. Salur,[49] J. Sandweiss,[49] M. Sarsour,[40] I. Savin,[13] P. S. Sazhin,[12] J. Schambach,[41] R. P. Scharenberg,[32] N. Schmitz,[23] K. Schweda,[21] J. Seger,[10] I. Selyuzhenkov,[47] P. Seyboth,[23] E. Shahaliev,[12] M. Shao,[37] W. Shao,[5] M. Sharma,[29] W. Q. Shen,[38] K. E. Shestermanov,[31] S. S. Shimanskiy,[12] E. Sichtermann,[21] F. Simon,[22] R. N. Singaraju,[44] N. Smirnov,[49] R. Snellings,[27] G. Sood,[43] P. Sorensen,[21] J. Sowinski,[17] J. Speltz,[18] H. M. Spinka,[1] B. Srivastava,[32] A. Stadnik,[12] T. D. S. Stanislaus,[43] R. Stock,[14] A. Stolpovsky,[47] M. Strikhanov,[25] B. Stringfellow,[32] A. A. P. Suaide,[36] E. Sugarbaker,[28] M. Sumbera,[11] B. Surrow,[22] M. Swanger,[10] T. J. M. Symons,[21] A. Szanto de Toledo,[36] A. Tai,[8] J. Takahashi,[36] A. H. Tang,[27] T. Tarnowsky,[32] D. Thein,[8] J. H. Thomas,[21] A. R. Timmins,[3] S. Timoshenko,[25] M. Tokarev,[12] T. A. Trainor,[46] S. Trentalange,[8] R. E. Tribble,[40] O. D. Tsai,[8] J. Ulery,[32] T. Ullrich,[4] D. G. Underwood,[1] G. Van Buren,[4] N. van der Kolk,[27] M. van Leeuwen,[21] A. M. Vander Molen,[24] R. Varma,[16] I. M. Vasilevski,[13] A. N. Vasiliev,[31] R. Vernet,[18] S. E. Vigdor,[17] Y. P. Viyogi,[44] S. Vokal,[12] S. A. Voloshin,[47] W. T. Waggoner,[10] F. Wang,[32] G. Wang,[20] G. Wang,[5] X. L. Wang,[37] Y. Wang,[41] Y. Wang,[42] Z. M. Wang,[37] H. Ward,[41] J. W. Watson,[20] J. C. Webb,[17] G. D. Westfall,[24] A. Wetzler,[21] C. Whitten Jr.,[8] H. Wieman,[21] S. W. Wissink,[17] R. Witt,[2] J. Wood,[8] J. Wu,[37] N. Xu,[21] Z. Xu,[4] Z. Z. Xu,[37] E. Yamamoto,[21] P. Yepes,[35] I-K. Yoo,[33] V. I. Yurevich,[12] I. Zborovsky,[11] H. Zhang,[4] W. M. Zhang,[20] Y. Zhang,[37] Z. P. Zhang,[37] C. Zhong,[38] R. Zoulkarneev,[13] Y. Zoulkarneeva,[13] A. N. Zubarev,[12] and J. X. Zuo[38]

(STAR Collaboration)

[1]*Argonne National Laboratory, Argonne, Illinois 60439, USA*

[2]*University of Bern, 3012 Bern, Switzerland*

[3]*University of Birmingham, Birmingham, United Kingdom*

[4]*Brookhaven National Laboratory, Upton, New York 11973, USA*

[5]*California Institute of Technology, Pasadena, California 91125, USA*

[6]*University of California, Berkeley, California 94720, USA*

[7]*University of California, Davis, California 95616, USA*

[8]*University of California, Los Angeles, California 90095, USA*
[9]*Carnegie Mellon University, Pittsburgh, Pennsylvania 15213, USA*
[10]*Creighton University, Omaha, Nebraska 68178, USA*
[11]*Nuclear Physics Institute AS CR, 250 68 Řež/Prague, Czech Republic*
[12]*Laboratory for High Energy (JINR), Dubna, Russia*
[13]*Particle Physics Laboratory (JINR), Dubna, Russia*
[14]*University of Frankfurt, Frankfurt, Germany*
[15]*Institute of Physics, Bhubaneswar 751005, India*
[16]*Indian Institute of Technology, Mumbai, India*
[17]*Indiana University, Bloomington, Indiana 47408, USA*
[18]*Institut de Recherches Subatomiques, Strasbourg, France*
[19]*University of Jammu, Jammu 180001, India*
[20]*Kent State University, Kent, Ohio 44242, USA*
[21]*Lawrence Berkeley National Laboratory, Berkeley, California 94720, USA*
[22]*Massachusetts Institute of Technology, Cambridge, Massachusetts 02139-4307, USA*
[23]*Max-Planck-Institut für Physik, Munich, Germany*
[24]*Michigan State University, East Lansing, Michigan 48824, USA*
[25]*Moscow Engineering Physics Institute, Moscow Russia*
[26]*City College of New York, New York City, New York 10031, USA*
[27]*NIKHEF and Utrecht University, Amsterdam, The Netherlands*
[28]*Ohio State University, Columbus, Ohio 43210, USA*
[29]*Panjab University, Chandigarh 160014, India*
[30]*Pennsylvania State University, University Park, Pennsylvania 16802, USA*
[31]*Institute of High Energy Physics, Protvino, Russia*
[32]*Purdue University, West Lafayette, Indiana 47907, USA*
[33]*Pusan National University, Pusan, Republic of Korea*
[34]*University of Rajasthan, Jaipur 302004, India*
[35]*Rice University, Houston, Texas 77251, USA*
[36]*Universidade de Sao Paulo, Sao Paulo, Brazil*
[37]*University of Science & Technology of China, Anhui 230027, China*
[38]*Shanghai Institute of Applied Physics, Shanghai 201800, China*
[39]*SUBATECH, Nantes, France*
[40]*Texas A&M University, College Station, Texas 77843, USA*
[41]*University of Texas, Austin, Texas 78712, USA*
[42]*Tsinghua University, Beijing 100084, China*
[43]*Valparaiso University, Valparaiso, Indiana 46383, USA*
[44]*Variable Energy Cyclotron Centre, Kolkata 700064, India*
[45]*Warsaw University of Technology, Warsaw, Poland*
[46]*University of Washington, Seattle, Washington 98195, USA*
[47]*Wayne State University, Detroit, Michigan 48201, USA*
[48]*Institute of Particle Physics, CCNU (HZNU), Wuhan 430079, China*
[49]*Yale University, New Haven, Connecticut 06520, USA*
[50]*University of Zagreb, Zagreb, HR-10002, Croatia*

(Received 2 November 2005; published 8 December 2006)

We report on p-Λ, p-$\overline{\Lambda}$, $\overline{p}$-Λ, and $\overline{p}$-$\overline{\Lambda}$ correlation functions constructed in central Au-Au collisions at $\sqrt{s_{NN}} = 200$ GeV by the STAR experiment at RHIC. The proton and lambda source size is inferred from the p-Λ and $\overline{p}$-$\overline{\Lambda}$ correlation functions. It is found to be smaller than the pion source size also measured by the STAR experiment at smaller transverse masses, in agreement with a scenario of a strong universal collective flow. The p-$\overline{\Lambda}$ and $\overline{p}$-Λ correlation functions, which are measured for the first time, exhibit a large anticorrelation. Annihilation channels and/or a negative real part of the spin-averaged scattering length must be included in the final-state interactions calculation to reproduce the measured correlation function.

DOI: 10.1103/PhysRevC.74.064906 PACS number(s): 25.75.Gz

I. INTRODUCTION

Correlations among nonidentical particles are sensitive to the space-time extent of their emitting source (see, e.g., [1]). Originally uncorrelated particles produced in nearby phase space points in the prompt emission final state can interact

through the nuclear and/or the Coulomb force and become correlated at time scales much longer than the production time. When the final-state interaction (FSI) is relatively well understood the emitting source size can be inferred from correlations at small relative three-velocity of the particles in their center-of-mass system. In relativistic heavy-ion collisions large particle densities are produced and the collision fireball may undergo a collective expansion (i.e., flow) [2,3]. This flow can induce space-momentum correlation so that particles with similar velocities come from the nearby regions of the source. With a strong flow at RHIC, as suggested by several measurements (see, e.g., Refs. [2–5]), the observed source sizes should be reduced relative to a source without flow [29] and vary with the mass of the emitted particle: the heavier the particle, the smaller is the reduction of the collective flow effect due to the thermal motion and the smaller are the apparent source sizes [5,6]. This flow effect can also be studied with p-p correlations and compared with π-π or K-K correlations. As compared with the p-p system, the p-Λ system gains in statistics in the region of small relative velocities due to the absence of repulsive Coulomb interaction [7].

In this article we test the hypothesis that a strong flow is established in Au+Au collisions at $\sqrt{s_{NN}} = 200$ GeV by comparing the source sizes of protons and lambdas to that of pions. The first measurements of $\overline{p}$-Λ, p-$\overline{\Lambda}$, and $\overline{p}$-$\overline{\Lambda}$ correlation functions are presented. The p-Λ and $\overline{p}$-$\overline{\Lambda}$ interaction potentials are relatively well understood, so we are able to infer source sizes [6–11]. The $\overline{p}$-Λ and p-$\overline{\Lambda}$ FSI, however, are unknown. As such, the scattering lengths and source sizes are extracted by fitting the data from the STAR experiment with the Lednický and Lyuboshitz analytical model [12]. In addition to constraining baryon-antibaryon potentials, this information determines unknown $\overline{p}$-Λ and p-$\overline{\Lambda}$ annihilation cross sections that are useful to constrain heavy-ion cascade models [13].

II. DATA RECONSTRUCTION

A. Events selection

The analysis was carried out using the STAR detector at RHIC [14]. Two million Au+Au collisions have been analyzed with $\sqrt{s_{NN}} = 200$ GeV. Because of statistics issues, only the 10% most central collisions were selected with the zero-degree calorimeters and the central trigger barrel of the STAR detector. This event selection procedure is explained in detailed in Ref. [5]. The other centrality selections gave no statistically meaningful results. Tracking of charged particles was accomplished using the STAR Time Projection Chamber (TPC), which covers the kinematic range of transverse momentum $p_t > 150\,\mathrm{MeV}/c$, pseudorapidity $|\eta| < 1.5$, and azimuthal angle $0 < \phi < 2\pi$. Events analyzed in this article have collision vertices within ±25 cm longitudinally of the TPC center.

B. Protons and antiprotons selection

Protons and antiprotons are identified using their specific energy loss (dE/dx) in the TPC gas. This selection limits the acceptance of particles to the transverse-momentum range of 0.4–1.1 GeV/c in the rapidity interval $|y| < 0.5$. Tracks pointing to within 3 cm of the primary vertex are included in the primary track sample.

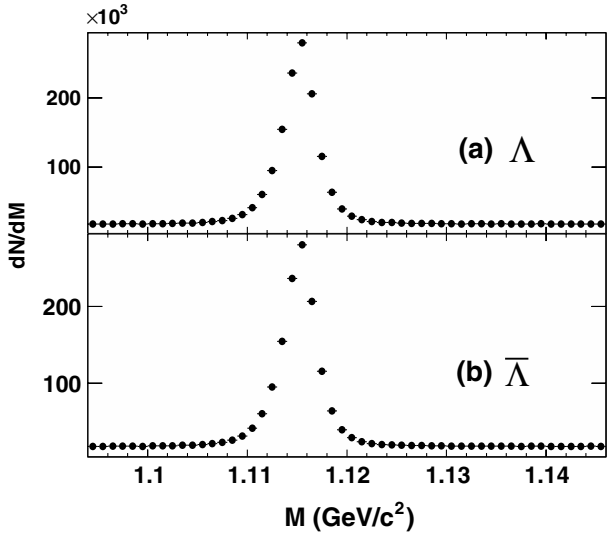

FIG. 1. Invariant mass of the selected Λ (a) and $\overline{\Lambda}$ (b) background not substracted with $0.3 < p_t < 2.0\,\mathrm{GeV}/c$. The y axis represents the number of candidates used in this analysis.

C. Lambdas and antilambdas selection

Lambdas (antilambdas) are reconstructed through the decay channel $\Lambda \to \pi^- + p(\overline{\Lambda} \to \pi^+ + \overline{p})$ [15], with a branching ratio of 64%. Pions and protons (i.e., lambda daughters) are selected using their specific energy loss. The invariant mass (Fig. 1) range of the lambda candidates is $1115 \pm 6\,\mathrm{MeV}/c^2$, the $\pm 6\,\mathrm{MeV}/c^2$ has been fixed to optimize the signal-over-noise ratio. The signal-over-noise ratio is equal to $86 \pm 6\%$ for lambda ($\langle p_t \rangle = 1.05\,\mathrm{GeV}/c$) and for antilambda ($\langle p_t \rangle = 1.09\,\mathrm{GeV}/c$) in the $\pm 6\,\mathrm{MeV}/c^2$ mass window and $0.3 < p_t < 2.0\,\mathrm{GeV}/c$. The correlation effect was the same within the errors with one sigma cut ($\pm 3\,\mathrm{MeV}/c^2$) on the invariant mass. In addition the following geometrical cuts are applied. The distance of the closest approach (DCA) of lambda daughters is required to be less than 0.7 cm. The DCA of the decay pions with respect to the primary vertex is required to be greater than 2.0 cm. The DCA of the reconstructed neutral particles to the primary vertex is required to be less than 0.6 cm. To avoid K^0_S being misidentified as lambdas, lambda candidates are rejected if their invariant mass is within the window $497.7^{+10.0}_{-21.3}\,\mathrm{MeV}/c^2$ when the pion mass is assumed for the two daughters. Due to the detector acceptance and the selection criteria, the p_t range of the lambda sample is $0.3 < p_t < 2.0\,\mathrm{GeV}/c$ and $|y| < 1.5$.

D. Pairs selection

When studying two-particle FSI, the relevant variable is the momentum of one of the particles in the pair rest frame called here $\vec{k}^*(k^* = |\vec{k}^*|)$. The correlation function has been extracted by constructing the ratio of two distributions. The numerator is the k^* distribution of pairs from the same event.

The denominator is the k^* distribution of pairs composed of particles from different events with primary vertices separated from each other by less than 10 cm. The ratio is formed by dividing the numerator by the denominator. Then the ratio is normalized to 1 at high k^* ($k^* > 0.35\,\mathrm{GeV}/c$). The event mixing procedure is the same as the one used in Ref. [5]. When reconstructing a primary lambda (antilambda) the decay proton (antiproton) points directly back to the primary vertex and may share some hits with a primary proton (antiproton) in the TPC. This phenomenon is called track merging and can occur while building pairs for the correlation function. In case of track merging, instead of counting two tracks with small k^* only one track will be found. So one pair will be missed at small k^*. If a lot of pairs are missed, the correlation function will show a hole at small k^* because they are not found. A missed pair leads to a fake correlation because of the event mixing procedure. A pair can be missed in a real event (in the numerator). Such a pair may be reconstructed taking two different events to build the background (in the denominator). Thus, track merging leads to fake correlations. For two tracks of different momenta, or different polar angles, the number of shared hits may vary as a function of where they cross in the TPC. It could be as low as 5 hits on the edge of the TPC. The tracker cannot find these hits, it is linked with the finding seed. This affects high p_t tracks because they will have more hits merged. To avoid such fake correlations, track merging has been studied for all other possible track-daughter track combinations. The study of track merging for lambda daughters and proton/antiproton tracks leads to two different selections criteria. The first selection requires tracks to share fewer than 10% of their TPC space points. The second selection deals with the average separation between primary tracks and lambda/antilambda daughter tracks. The track separation is calculated as an arithmetic mean distance between the TPC hits of the two tracks for a given radius. If a track crosses the whole TPC, it will be reconstructed with a maximum of 45 hits. Because one of the lambda/antilambda daughter tracks is a secondary track, all 45 hits of the TPC may not be available, so the mean is calculated from a maximum of 11 distances. In this article "secondary particles" means particle from decay. As a consequence the average separation between protons/antiprotons and lambda/antilambda daughters are required to be greater than 11 cm for $\overline{p}$-$\overline{p}_{\overline{\Lambda}}$, $\overline{p}$-p_Λ, $\overline{p}$-π_Λ, and p-$\pi_{\overline{\Lambda}}$; 10 cm for p-p_Λ; 12 cm for $\overline{p}$-$\overline{p}_{\overline{\Lambda}}$; and 17 cm for p-π_Λ and $\overline{p}$-$\pi_{\overline{\Lambda}}$. The first selection prevents interference between opposite sign tracks that, even though their average separation is large, can cross each other in the TPC. When the trajectories of the particles cross, space points can be assigned to the wrong track during reconstruction. In some cases this can lead to a failure to reconstruct one of the tracks. For this reason the values for the minimum average separation are larger for opposite sign pairs.

III. PURITY

A. Definition

Impurities in the sample of protons and lambdas will reduce the observed p-Λ correlation strength. In the case of lambdas, fake lambda candidates (from combinatorial background) and secondary lambdas (e.g., from Σ^0 decays) are the two main sources of impurity. The sample of protons is contaminated by other charged tracks falsely identified as protons and by protons from weak decays (feed-down). To correct the observed correlations for misidentification and feed-down we estimate the particle purity for p, $\overline{p}$, Λ, and $\overline{\Lambda}$ as a function of transverse momentum (p_t):

TABLE I. Summary of the particle purity due to identifications and weak-decay contamination. Values are averaged over the transverse momentum without taking into account the transverse momentum dependence for $k^* < 0.2\,\mathrm{GeV}/c$.

Particle	Identification	Fraction primary
p	$76 \pm 7\%$	$52 \pm 4\%$
$\overline{p}$	$74 \pm 7\%$	$48 \pm 4\%$
Λ	$86 \pm 6\%$	$45 \pm 4\%$
$\overline{\Lambda}$	$86 \pm 6\%$	$45 \pm 4\%$

$$\mathrm{ParticlePurity}(p_t) = \mathrm{Pid}(p_t) \times \mathrm{Fp}(p_t), \tag{1}$$

where Pid is *the probability a candidate was correctly identified* and Fp is *the fraction of the candidates that were primary particles*. The final correction depends on the product of the particle purity for both particles (i.e, the PairPurity). The pair impurity is corrected for in constructing the correlation function in k^*.

The feed-down estimations have been done for p, $\overline{p}$, Λ, and $\overline{\Lambda}$ and are summarized in Table I. Combined results from STAR [2,3,16,17] and predictions from a thermal model [18–20] have been used. The approximations introduced by estimating the purity are the major source of systematic uncertainties on the extracted values of FSI parameters and source radii discussed below.

B. Protons and antiprotons purities

The identification probabilities have been estimated for charged particles; they are also given in Table I. A track can be identified as a pion, a kaon, a proton/antiproton, and an electron/positron with a certain probability using the information about the energy loss dE/dx [21]. Identified protons (antiprotons) from the selected sample have a mean identification probability of $76 \pm 7\%$ ($74 \pm 7\%$). This mean identification probability and the corresponding p_t are calculated over all selected tracks considered as protons (antiprotons). The calculated feed-down leads to a mean estimated fraction of primary protons of 52% [with a mean transverse velocity $\langle\beta_t\rangle \equiv \langle p_t/\gamma\rangle/m) = 0.58$, m is the mass of the particle]. Most of the secondary protons come from lambda decays (primary Λ and Λ from Σ^0, Ξ^0, and Ξ^-) and constitute 36% of the protons used to construct the correlation function. Other sources of contamination for protons are products of Σ^+ decays and interactions of pions with detector materials that represent, respectively, 10 and 2% of the sample. The feed-down study for antiprotons ($\langle\beta_t\rangle = 0.60$) leads to an estimated fraction of primary antiprotons of 48%. Most of

the secondary antiprotons come from antilambda decay (primary $\overline{\Lambda}$ and $\overline{\Lambda}$ from $\overline{\Sigma^0}$, $\overline{\Xi^0}$, and $\overline{\Xi^-}$) and constitute 39% of the antiprotons used to construct the correlation function. Antiprotons from $\overline{\Sigma^+}$ decays are another major source of contamination; they make up 13% of the antiproton sample.

C. Lambdas and antilambdas purities

For lambdas and antilambdas the probability of misidentification corresponds to background estimation under the mass peak. The corresponding identification probabilities are practically independent of p_t and equal to $86 \pm 6\%$ for both lambdas and antilambdas, respectively. The sample of lambdas (antilambdas) includes secondary particles such as decay products of Ξ^-, Ξ^0, Σ^0 ($\overline{\Xi^-}$, $\overline{\Xi^0}$, $\overline{\Sigma^0}$). The fractions of primary lambdas ($\langle\beta_t\rangle = 0.68$) and primary antilambdas ($\langle\beta_t\rangle = 0.70$) have been estimated at 45%.

D. Pairs purities

The pair purity plays a crucial role in the correlation study. The estimated value of the mean pair purity for p-Λ, $\overline{p}$-$\overline{\Lambda}$, p-$\overline{\Lambda}$, and $\overline{p}$-Λ systems is $\lambda = 17.5 \pm 2.5\%$ after taking into account the transverse-momentum dependence. Without taking into account the transverse momentum dependence the estimated purities differ by 2% (Table I).

IV. CORRECTIONS

A. Purity

Because the contamination reduces the correlation strength, raw data have been corrected for purity using the relation:

$$C^{\text{corr}}_{\text{measured}}(k^*) = \frac{C_{\text{measured}}(k^*) - 1}{\text{PairPurity}} + 1, \qquad (2)$$

where PairPurity is the product of the purities for the two particles and $C^{\text{corr}}_{\text{measured}}(k^*)$ and $C_{\text{measured}}(k^*)$ are respectively the corrected and measured correlation functions. Equation (2) assumes that misidentified and weak decay protons (antiprotons) are uncorrelated with lambdas and antilambdas. This assumption is justified for misidentified protons (antiprotons) because the eventual pion or kaon correlation at small k^* is washed out after the wrong mass assignment. Combinatoric background reconstructed as Λ and $\overline{\Lambda}$ also leads to uncorrelated pairs. However, weak decay products may keep a residual correlation from their parents. This assumption will be revisited when extracting source sizes and scattering lengths from the correlation functions.

B. Momentum resolution

The effects of momentum resolution have been studied using mixed pairs by calculating the weight with the Lednický and Lyuboshitz analytical model [12]. It appears that compared with statistical and systematic errors, the impact of the momentum resolution effect is negligible. Indeed, the momentum resolution effect leads to about 1% variation of the apparent source radius. Nevertheless, correlation functions have been corrected for the momentum resolution using the following formula:

$$C_{\text{true}}(k^*) = \frac{C^{\text{corr}}_{\text{measured}}(k^*) \times C_{\text{Th-not-smeared}}(k^*)}{C_{\text{Th-smeared}}(k^*)}, \qquad (3)$$

where $C_{\text{true}}(k^*)$ represents the corrected correlation function, $C_{\text{Th-not-smeared}}(k^*)/C_{\text{Th-smeared}}(k^*)$ is the correction factor; $C_{\text{Th-not-smeared}}(k^*)$ is calculated without taking into account the effect of momentum resolution, and $C_{\text{Th-smeared}}(k^*)$ includes this effect. The shift due to the momentum resolution is studied using simulated tracks introduced into real events. This shift is applied to momenta to calculate $C_{\text{Th-smeared}}(k^*)$.

V. RESULTS

A. Correlation functions

In Fig. 2(a) the corrected p-Λ and $\overline{p}$-$\overline{\Lambda}$ correlation functions are shown. They are close to each other, within error bars, showing a pair excess at small k^* ($0 < k^* < 0.1\,\text{GeV}/c$) indicating an attractive potential between (anti-)proton and (anti-)lambda. Figure 2(b) shows the corrected $\overline{p}$-Λ and p-$\overline{\Lambda}$ correlation functions measured for the first time. They are below unity in a wide k^* range $0 < k^* < 0.25\,\text{GeV}/c$ consistent with positive imaginary parts of the s-wave scattering lengths (due to the open annihilation channels) and a negative real part of the spin averaged s-wave scattering length. In Fig. 3 the combined $(p\text{-}\Lambda) \oplus (\overline{p}\text{-}\overline{\Lambda})$ and $(\overline{p}\text{-}\Lambda) \oplus (p\text{-}\overline{\Lambda})$ correlation functions are presented. The symbol ⊕ means that numerators and denominators of the systems have been added to build the combined correlation functions. In both figures, curves correspond to a fit carried out with the Lednický and Lyuboshitz analytical model [12].

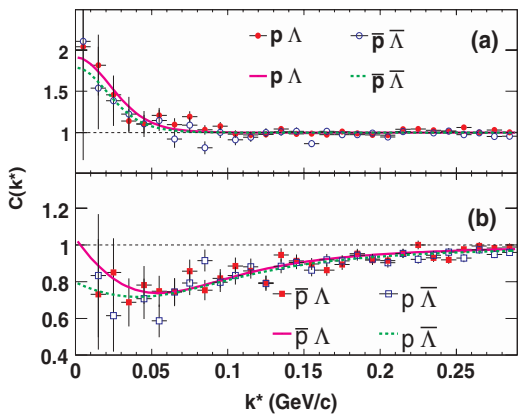

FIG. 2. (Color online) The purity and momentum-resolution corrected correlation functions $C_{\text{true}}(k^*)$ for p-Λ, $\overline{p}$-$\overline{\Lambda}$ (a), $\overline{p}$-Λ, p-$\overline{\Lambda}$ (b). Curves correspond to fits done using the Lednický and Lyuboshitz analytical model [12].

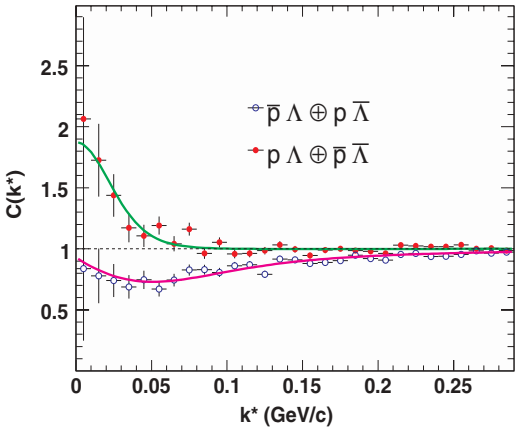

FIG. 3. (Color online) $(p\text{-}\Lambda) \oplus (\overline{p}\text{-}\overline{\Lambda})$ and $(\overline{p}\text{-}\Lambda) \oplus (p\text{-}\overline{\Lambda})$ combined correlation functions. Correlation functions are corrected for purity and momentum resolution. Curves correspond to fits done using the Lednický and Lyuboshitz analytical model [12].

B. Lednický and Lyuboshitz analytical model

This model relates the two-particle correlation functions with source sizes and scattering amplitudes [12,22]. As usual, similar to the Fermi factor in the theory of β decay, the correlation function $[C(k^*)]$ is calculated as the square of the wave function (Ψ^S) averaged over the total spin S and over the distribution of relative distance $(\vec{r^*})$ of particle emission points in the pair rest frame

$$C(k^*) = \left\langle \left| \Psi^S_{-\vec{k^*}}(\vec{r^*}) \right|^2 \right\rangle. \tag{4}$$

It should be noted that the two particles are generally produced at nonequal times in their center-of-mass system and that the wave function in Eq. (4) should be substituted by the Bethe-Salpeter amplitude. The latter depends on both space $(\vec{r^*})$ and time (t^*) separation of the emission points in the pair rest frame and at small $|t^*|$ coincides with the wave function Ψ^S up to a correction $\mathcal{O}(|t^*/\mathrm{mr}^{*2}|)$, where m is the mass of the lighter particle. It can be shown that Eq. (4) is usually valid better than to few percentages even for particles as light as pions [12,23]. The wave function Ψ^S represents a stationary solution of the scattering problem having at large distances r^* the asymptotic form of a superposition of the plane and outgoing spherical waves. It is approximated by the solution outside the range of the strong interaction potential taking into account, at the considered small k^* values, the s-wave part of the scattered wave only:

$$\Psi^S_{-\vec{k^*}}(\vec{r^*}) \doteq e^{-i\vec{k^*}\cdot\vec{r^*}} + \frac{f^S(k^*)}{r^*} e^{ik^*\cdot r^*}, \tag{5}$$

with the effective range approximation for the s-wave scattering amplitude:

$$f^S(k^*) = \left(\frac{1}{f_0^S} + \frac{1}{2} d_0^S k^{*2} - ik^* \right)^{-1}, \tag{6}$$

where f_0^S is the scattering length and d_0^S is the effective radius for a given total spin $S = 1$ or $S = 0$, i.e., for a triplet (t) or singlet (s) state, respectively. We assume that particles are produced unpolarized, i.e., $\rho_0 = 1/4$ of the pairs are in the singlet state and $\rho_1 = 3/4$ are in the triplet state. Then, assuming a Gaussian distribution in r^*,

$$d^3N/d^3r^* \sim e^{-\vec{r^*}^2/4r_0^2}, \tag{7}$$

where r_0 can be considered as the effective radius of the source, the correlation function can be calculated analytically [12]:

$$C(k^*) = 1 + \sum_S \rho_S \left[\frac{1}{2} \left| \frac{f^S(k^*)}{r_0} \right|^2 \left(1 - \frac{d_0^S}{2\sqrt{\pi} r_0} \right) + \frac{2\Re f^S(k^*)}{\sqrt{\pi} r_0} F_1(Qr_0) - \frac{\Im f^S(k^*)}{r_0} F_2(Qr_0) \right], \tag{8}$$

where $F_1(z) = \int_0^z dx e^{x^2 - z^2}/z$ and $F_2(z) = (1 - e^{-z^2})/z$. The leading correction to the correlation function $\mathcal{O}(|f_0^S|^2 d_0^S/r_0^3)$ is introduced in Eq. (8) to account for the deviation of the solution (5) from the true wave function inside the range of the strong interaction potential.

C. FSI parameters and source sizes

The p-Λ and $\overline{p}$-$\overline{\Lambda}$ interaction potentials are relatively well understood [6–11], which allows us to extract the source radius r_0 from the fit. The best fits are compared with the separate p-Λ and with the $\overline{p}$-$\overline{\Lambda}$ correlation functions in Fig. 2(a), and the combined one in Fig. 3. The scattering lengths ($f_0^s = 2.88$ fm, $f_0^t = 1.66$ fm) and effective radii ($d_0^s = 2.92$ fm, $d_0^t = 3.78$ fm) from Ref. [7] have been used for the p-Λ, $\overline{p}$-$\overline{\Lambda}$ correlation functions. The systematic errors on the radius introduced by the uncertainties on the scattering lengths have been estimated to be 0.2 fm assuming spin averaged FSI parameters with 5% uncertainty. The fit results are summarized in Table II. The three errors are, from left to right, the statistical errors and the systematic errors introduced by the uncertainty on the purity correction and on the scattering length for p-Λ and $\overline{p}$-$\overline{\Lambda}$ systems and on the uncertainty in the model for p-$\overline{\Lambda}$ and $\overline{p}$-Λ systems. One parameter is free while fitting the

TABLE II. Comparison of the radius of the source of particles for p-Λ, $\overline{p}$-$\overline{\Lambda}$, $\overline{p}$-Λ, p-$\overline{\Lambda}$ and combined systems. For STAR, the three errors are, from left to right, the statistical errors and the systematic errors introduced by the uncertainty on the purity correction and on the scattering length for p-Λ and $\overline{p}$-$\overline{\Lambda}$ systems and on the uncertainty in the model for p-$\overline{\Lambda}$ and $\overline{p}$-Λ systems. For NA49 [6] and E895 [22], the λ parameter represents the pair purity.

Exp.	System	r_0 (fm)
STAR	p-Λ	$2.97 \pm 0.34^{+0.19}_{-0.25} \pm 0.2$
STAR	$\overline{p}$-$\overline{\Lambda}$	$3.24 \pm 0.59^{+0.24}_{-0.14} \pm 0.2$
STAR	p-$\Lambda \oplus \overline{p}$-$\overline{\Lambda}$	$3.09 \pm 0.30^{+0.17}_{-0.25} \pm 0.2$
STAR	$\overline{p}$-Λ	$1.56 \pm 0.08^{+0.10}_{-0.14} \pm 0.3$
STAR	p-$\overline{\Lambda}$	$1.41 \pm 0.10 \pm 0.11 \pm 0.3$
STAR	$\overline{p}$-$\Lambda \oplus p$-$\overline{\Lambda}$	$1.50 \pm 0.05^{+0.10}_{-0.12} \pm 0.3$
NA49	p-Λ ($\lambda = 0.33$ fixed)	3.8 ± 0.33
NA49	p-Λ ($\lambda = 0.17 \pm 0.11$ free)	2.9 ± 0.7
E895	p-Λ ($\lambda = 0.5 \pm 0.2$ free)	4.5 ± 0.7

p-Λ, the $\overline{p}$-$\overline{\Lambda}$, and the combined correlation functions. Three parameters are free while fitting the p-$\overline{\Lambda}$, the $\overline{p}$-Λ, and for the combined correlation functions. Statistical errors on the radii are larger for the p-Λ, the $\overline{p}$-$\overline{\Lambda}$, and the combined correlation functions than for the corresponding baryon-antibaryon ones. The p-$\overline{\Lambda}$, the $\overline{p}$-Λ, and the combined correlation functions have a large width and involve more statistics in the fit of the correlated k^* region as compared with the p-Λ, the $\overline{p}$-$\overline{\Lambda}$, and the combined correlation functions.

The extracted source radii are close to the values (3–4 fm) obtained in measurements performed by the NA49 (SPS) Collaboration in Pb+Pb collisions at 158A GeV [6] and by the E895 (AGS) experiment in Au+Au collisions at 4, 6, and 8A GeV [8,22]. This confirms that the particle emitting source size does not change significantly with beam energy; a result also obtained by studying two-pion correlations.

The $\overline{p}$-Λ and p-$\overline{\Lambda}$ scattering lengths have never been measured before. Hence, they have to be included as free parameters in the fit to the experimental correlation functions. To limit the number of free parameters, the following assumptions are made: (i) the spin dependence is neglected, $f^s = f^t = f$, and (ii) the effective radius (d_0) is set to zero. An extra parameter Im $f_0 > 0$ is added, taking into account the annihilation channels.

The best fits are compared with the separate $\overline{p}$-Λ and p-$\overline{\Lambda}$ correlation functions in Fig. 2(b) and with the combined one in Fig. 3. The fitted spin-averaged scattering lengths for the combined p-$\overline{\Lambda}$ and $\overline{p}$-Λ systems are compared with measurements for the p-$\overline{p}$ system [24–27] in Fig. 4. The imaginary part of the fitted scattering length is in agreement with the p-$\overline{p}$ results, whereas the real part is more negative. The error contour represents the statistical errors. The systematic error due to the uncertainty on pair purity is investigated by comparing the best estimated k^*-dependent purity with k^*-independent purity corrections λ. The k^*-dependent purity correction tends to decrease the size of the error contour (the curve labeled Corrected) as compared with

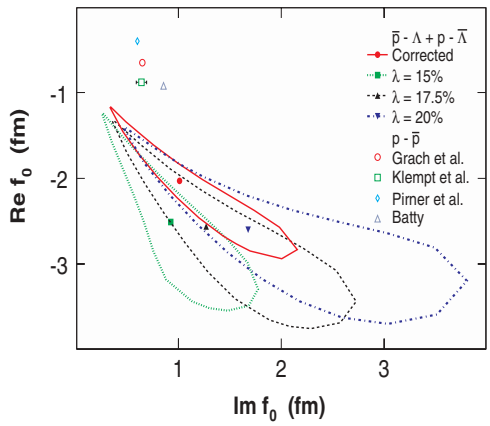

FIG. 4. (Color online) The combined $(\overline{p}\text{-}\Lambda) \oplus (p\text{-}\overline{\Lambda})$ spin-averaged s-wave scattering length compared with the previous measurements for the p-$\overline{p}$ system [24–27]. The curves show the one standard deviation contours. Note that for $(\overline{p}\text{-}\Lambda) \oplus (p\text{-}\overline{\Lambda})$ only, one should read $0.1973 \times \mathrm{Im}\, f_0$ instead of $\mathrm{Im}\, f_0$ on the x-axis.

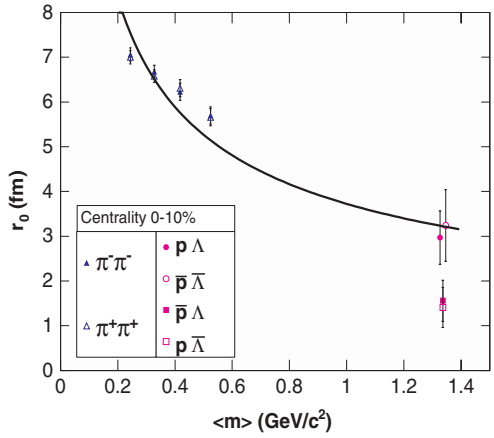

FIG. 5. (Color online) Pion source size [5] compared with proton and lambda source sizes as a function of the mean transverse mass ($\langle m_t \rangle$). The curve shows the $\langle m_t \rangle^{-1/2}$ dependence with an arbitrary normalization.

the one for the constant purity (the curve labeled $\lambda = 17.5\%$) and shifts both the real and imaginary parts of the scattering length in the direction of the p-$\overline{p}$ values.

The radii extracted from the fits to the separate and the combined p-$\overline{\Lambda}$ and $\overline{p}$-Λ correlation functions are summarized in Table II. The errors include from left to right, statistical errors, systematic errors due to purity, and systematic errors estimated from varying model parameters. The error on the radius parameter due to the uncertainties on the model is estimated to be 0.3 fm. This error is estimated by fixing the spin-averaged scattering lengths and by extracting the radius and the effective radius. For the moment, we do not have any tool to extract the radius uncertainty related to the neglected p-wave contribution. A larger radius implies a correlation over a smaller k^* range than seen in the data, which cannot be recovered by increasing the magnitude of scattering lengths. However, the radii extracted from the p-Λ (and $\overline{p}$-$\overline{\Lambda}$) and the $\overline{p}$-Λ (and p-$\overline{\Lambda}$) are significantly different. The error bars accounting for all statistic and systematic contributions barely overlap.

VI. DISCUSSION

The difference in radii between p-Λ ($\overline{p}$-$\overline{\Lambda}$) and $\overline{p}$-Λ (p-$\overline{\Lambda}$) is unexpected. Indeed, it would imply a novel dynamical space-momentum correlation between proton ($\overline{p}$) and $\overline{\Lambda}$ (Λ). Strong space-momentum correlations are exhibited in Au+Au collisions at RHIC. These are understood to arise from the collective flow of massive particles [5,28]. This effect, however, would not lead to a difference between the source size measured from p-Λ and $\overline{p}$-Λ correlations. In Fig. 4, the source sizes from proton-Lambda correlations and pion-pion correlations are plotted as a function of the mean of the particles' transverse masses. The decrease of the source size with increasing mean transverse mass is in qualitative agreement with expectations from collective flow [29]. The curve in Fig. 5 represents an arbitrarily normalized $\langle m_t \rangle^{-1/2}$ dependence. This dependence is expected within some hydrodynamics-motivated models [30]. The data are

TABLE III. Summary of the main fractions of pairs containing particles from particle decays included in p-Λ, p-$\overline{\Lambda}$, $\overline{p}$-Λ, and $\overline{p}$-$\overline{\Lambda}$ correlation functions assuming the absence of residual correlations. Λ_Ξ are Λ ($\overline{\Lambda}$) decay products of Ξ^-, Ξ^0 ($\overline{\Xi^-}$, $\overline{\Xi^0}$), Λ_{Σ^0}, are Λ ($\overline{\Lambda}$) decay products of Σ^0 ($\overline{\Sigma^0}$), p_Λ are p ($\overline{p}$) decay products of Λ ($\overline{\Lambda}$), p_{Σ^+} are p ($\overline{p}$) decay products of Σ^+ ($\overline{\Sigma^+}$), Λ_{prim} and p_{prim} represent primary Λ ($\overline{\Lambda}$) and p ($\overline{p}$). The remaining 29% represents misidentified p ($\overline{p}$) and reconstructed fake Λ ($\overline{\Lambda}$).

Pairs	Fractions (%)
p_{prim}-Λ_{prim}	15
p_Λ-Λ_{prim}	10
p_{Σ^+}-Λ_{prim}	3
p_{prim}-Λ_{Σ^0}	11
p_Λ-Λ_{Σ^0}	7
p_{Σ^+}-Λ_{Σ^0}	2
p_{prim}-Λ_Ξ	9
p_Λ-Λ_Ξ	5
p_{Σ^+}-Λ_Ξ	2
p_{prim}-p_{prim}	7

in reasonable agreement with this expectation. In addition, a possible difference between radii pointed by data may imply that baryon- anti-baryon pairs are produced close in space, a dynamic correlation that is not in baryon-baryon pairs.

Although a novel space-momentum correlation between proton and $\overline{\Lambda}$ cannot be ruled out, the difference between the radii extracted from p-Λ and $\overline{p}$-Λ correlation functions may come from an imperfect treatment of the purity correction. Indeed, we have assumed that any pairs that are not composed of two primary particles are not correlated. However, Table III shows that a number of such pairs may carry a residual correlation from their parents [31]. For example, the interaction between a primary proton and a Σ^0 may not be completely washed out when constructing the p-Λ correlation function with the Λ being the Σ^0 daughter as the Λ carries most of the momentum of its parent. This effect was found to be on the order of 10% [32]. However, none of the interactions between the pairs listed in Table III are known. We are thus unable to perform any reliable correction or error estimate. At that stage, we show the p-$\overline{\Lambda}$ and $\overline{p}$-Λ correlation function corrected with the best estimate of the purity assuming no residual correlations. We extract source radii and scattering length parameters acknowledging that the values may be biased by the presence of residual correlations.

VII. CONCLUSION

Constructing p-Λ, p-$\overline{\Lambda}$, $\overline{p}$-Λ, $\overline{p}$-$\overline{\Lambda}$, we have gathered information about the space-time features of baryon and antibaryon emission and about the interaction in p-$\overline{\Lambda}$ and $\overline{p}$-Λ systems. The source radii extracted from p-Λ and $\overline{p}$-$\overline{\Lambda}$ corrrelation function agree with the flow expectation. The radii extracted from $\overline{p}$-Λ and p-$\overline{\Lambda}$ are significantly smaller. Final-state interactions parameters, such as spin averaged s-wave scattering length, have been extracted from $\overline{p}$-Λ and p-$\overline{\Lambda}$ correlation functions. The real part of the scattering length appears to be negative while the imaginary part is positive, the latter being required by the unitarity due to the open annihilation channels. These results demonstrate that correlation measurements can be used to study the two-particle strong interaction for particle combinations that are difficult to access by other means, including traditional scattering experiments.

ACKNOWLEDGMENTS

We thank the RHIC Operations Group and RCF at BNL and the NERSC Center at LBNL for their support. This work was supported in part by the HENP Divisions of the Office of Science of the U.S. Department of Education; the U.S. NSF; the BMBF of Germany; IN2P3, RA, RPL, and EMN of France; EPSRC of the United Kingdom; FAPESP of Brazil; the Russian Ministry of Science and Technology; the Ministry of Education and the NNSFC of China; IRP and GA of the Czech Republic, FOM of the Netherlands, DAE, DST, and CSIR of the Government of India; Swiss NSF; the Polish State Committee for Scientific Research; STAA of Slovakia, and the Korea Science and Engineering Foundation.

[1] R. Lednický, V. L. Lyuboshitz, B. Erazmus, and D. Nouais, Phys. Lett. **B373**, 30 (1996).
[2] J. Adams *et al.* (STAR), Phys. Rev. Lett. **92**, 112301 (2004).
[3] J. Adams *et al.* (STAR), Phys. Rev. Lett. **92**, 182301 (2004).
[4] J. Adams *et al.* (STAR), Phys. Rev. C **72**, 014904 (2005).
[5] J. Adams *et al.* (STAR), Phys. Rev. C **71**, 044906 (2005).
[6] C. Blume *et al.* (NA49), Nucl. Phys. **A715**, 55 (2003).
[7] F. Wang and S. Pratt, Phys. Rev. Lett. **83**, 3138 (1999).
[8] P. Chung *et al.* (E895), Phys. Rev. Lett. **91**, 162301 (2003).
[9] Th. A. Rijken, V. G. J. Stoks, and Y. Yamamoto, Phys. Rev. C **59**, 21 (1999).
[10] P. M. M. Maessen, Th. A. Rijken, and J. J. de Swart, Phys. Rev. C **40**, 2226 (1989).
[11] M. M. Nagels, Th. A. Rijken, and J. J. de Swart, Phys. Rev. D **20**, 1633 (1979).
[12] R. Lednický, V. L. Lyuboshitz, Yad. Fiz. **35**, 1316 (1982) [Sov. J. Nucl. Phys. **35**, 770 (1982)]; Proc. CORINNE 90 Nantes, France, edited by D. Ardouin (World Scientific, Singapore, 1990), p. 42.
[13] G. J. Wang *et al.*, Report No. WSU-NP-98-2; nucl-th/9807036.
[14] K. H. Ackermann *et al.* (STAR), Nucl. Phys. **A661**, 681c (1999); K. H. Ackermann *et al.* (STAR), Nucl. Instrum. Methods A **499**, 624 (2003).
[15] J. Adams *et al.* (STAR), Phys. Lett. **B567**, 167 (2003).
[16] C. Adler *et al.* (STAR), Phys. Rev. Lett. **89**, 092301 (2002).
[17] M. A. C. Lamont, Ph.D. thesis, University of Birmingham (2002).
[18] P. Braun-Munzinger and J. Stachel, Nucl. Phys. **A606**, 320 (1996).
[19] P. Braun-Munzinger, I. Heppe, and J. Stachel, Phys. Lett. **B465**, 15 (1999).

[20] P. Braun-Munzinger, D. Magestro, K. Redlich, and J. Stachel, Phys. Lett. **B518**, 41 (2001).
[21] C. Adler *et al*. (STAR), Phys. Rev. Lett. **87**, 182301 (2001).
[22] R. Lednický, Proceedings of the International Workshop on the Physics of the Quark-Gluon Plasma, Palaiseau, (2001); nucl-th/0112011.
[23] R. Lednický, Report No. DIRAC Note 2004–06, CERN, 27-11-2004; nucl-th/0501065.
[24] I. L. Grach, B. O. Kerbikov, and Yu.A. Simonov, Sov. J. Nucl. Phys. **48**, 609 (1988).
[25] C. J. Batty, Rep. Prog. Phys. **52**, 1165 (1989).
[26] H. J. Pirner, B. O. Kerbikov, and J. Mahalanabis, Z. Phys. A **338**, 111 (1991).
[27] E. Klempt, F. Bradamante, A. Martin, and J. M. Richard, Phys. Rep. **368**, 119 (2002).
[28] J. Adams *et al*. (STAR), Phys. Rev. Lett. **91**, 262302 (2003).
[29] F. Retière and M. A. Lisa, Phys. Rev. C **70**, 044907 (2004).
[30] B. Tomášik, U. A. Wiedmann, and U. Heinz, Nucl. Phys. **A663**, 753 (2000).
[31] A. V. Stavinsky *et al*., Rapport interne Subatech-2003-03 (2003).
[32] F. Wang, Phys. Rev. C **60**, 067901 (1999).